Face Recognition based on Binary Images for Link Selection

Sanghun Lee[1], Soochang Kim[2], Young-hoon Kim[2] and Chulhee Lee[1]
[1]*Electrical And Electronic Engineering, Yonsei University, 134 Shinchon-dong, Seodaemoon-gu, 120-749, Seoul, Republic of Korea*
[2]*Electronics and Telecommunications Research Institute, 161, Gajeong-dong, Yusong-gu, 305-700, Daejeon, Republic of Korea*

Keywords: Binary Image, Difference of Gaussian, Face Recognition, Image Registration, Link Selection, Scale Pyramid.

Abstract: A face recognition system which utilizes binary facial images and a bitwise similarity calculation method is proposed for link selection between mobile devices. As a pre-processing step, normalized differences of Gaussian and facial region estimation were used to handle illumination conditions. Binary images were used to extract facial feature sets that did not exceed 700 bytes. Scale pyramids and XNOR+AND similarity scores were used for fast feature matching between reference data sets and pre-processed test data. The proposed method achieved about an 85.9% recognition rate with a database that consisted of 135 facial images with various head poses, obtained by enrolling one reference data set per subject.

1 INTRODUCTION

Recent advances in communication technology and mobile devices have enabled the development of wireless communications such as Wireless Fidelity (O'sullivan et al., 1996), Near Field Communication (Zimmerman, 1996), etc. Modern mobile devices can access each other through compact, low-cost, low-power, secure and cordless communication systems. However, a problem with these devices is that initializing connections between mobile devices requires prior knowledge of the target device (e.g. a unique ID of that device). Suppose that Alice wants to connect Bob's smartphone using Bluetooth. Alice first needs to turn on the Bluetooth mode and find the name of Bob's device on her mobile display. Although this is a reliable and secure way to connect wirelessly, it is not intuitive. In the proposed link selection system, Alice can connect by manually selecting Bob's face on her display. Since Bob's face is used as his ID, Alice doesn't have to ask him about anything or even remember an unfamiliar nickname. The only thing she has to do is to select a target on her display that shows a number of objects.

To use this link selection method, each mobile device broadcasts a feature set of its owner's face. This feature set can be used for recognizing the device by another device, which receives and compares the feature set with a selected facial area. Second, each feature set has a limited data size. In most protocols, there is a limit on the size of the broadcasting signals and we set the data size of this feature set not to exceed 700 bytes (as a requirement of communication channel capacity). Third, we assumed the device was also receiving signals from several neighboring devices at the same time, so it had to search the target device by matching the selected facial area and the received feature sets of broadcasted signals. Finally, we assumed that the computing power of each device was relatively low compared to that of a desktop computer. Consequently, the matching algorithm could not be a complex one. Thus, the main purpose of our research was to develop a face recognition system requiring a small amount of channel capacity (under 700 bytes) by using binary images for the link selection application.

2 OVERVIEW OF THE METHOD

The proposed system is shown in Fig. 1. The pre-processing chain discussed in earlier research (Tan and Triggs, 2007), which computes a normalized difference of Gaussian (DoG), was used to produce illumination-invariant facial images. We applied

Lee S., Kim S., Kim Y. and Lee C..
Face Recognition based on Binary Images for Link Selection.
DOI: 10.5220/0004738605890593
In *Proceedings of the 9th International Conference on Computer Vision Theory and Applications* (VISAPP-2014), pages 589-593
ISBN: 978-989-758-004-8

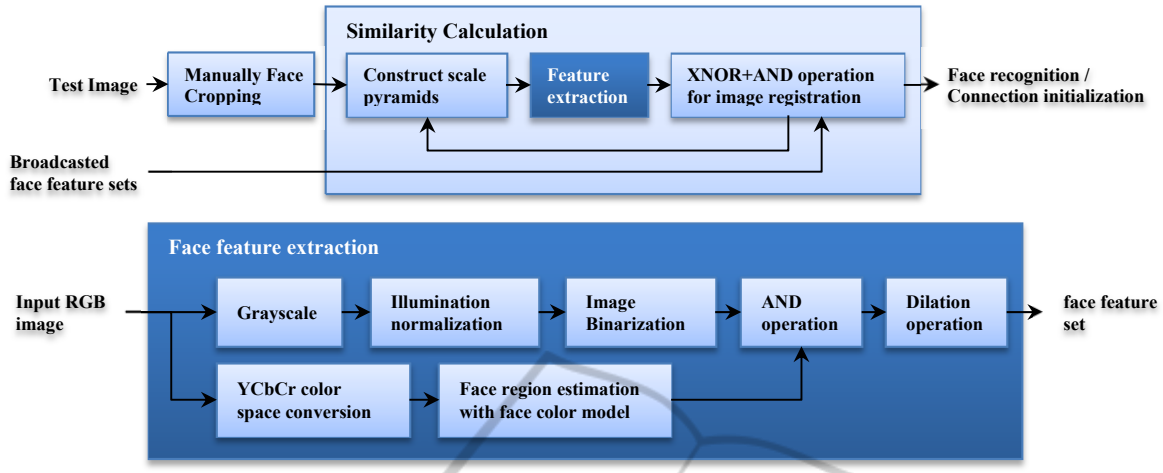

Figure 1: The proposed method consists of pre-processing, similarity calculation and decision steps.

additional facial region estimation by using a skin colour model (Chai and Ngan, 1999) in the YCbCr colour space, as well as global intensity shift and binary result images to obtain pose-invariant facial images. Each device stored a binary image of the owner's face (i.e. a reference image) and broadcasted this image as a feature set. This pre-processing step was applied to both reference and test images. The manually selected facial area was used as a test image. Since the reference image size was fixed due to the data size limitation, the sizes of the reference images and test image differed. Therefore, using the sliding window scheme (Colmenarez and Huang, 1997), image registration was performed at multiple scales to find the largest correlation score. Then, we chose the device that provided the highest score. The broadcasting signals also contained communication ID information such as IP addresses. This information was used to initialize the link between the two devices.

3 FACE FEATURE EXTRATION

3.1 Illumination Normalization

Various illumination conditions and camera settings can affect overall face recognition performance. Since the proposed matching algorithm was used to directly compare the features of a test image in a pixel-wise manner with those of a reference image, essential facial features had to be preserved while compensating for the illumination effects. The pre-processing method was applied to gray-scale facial images for illumination normalization. It consisted of gamma correction, difference of Gaussian filters and contrast equalization (Fig. 2b).

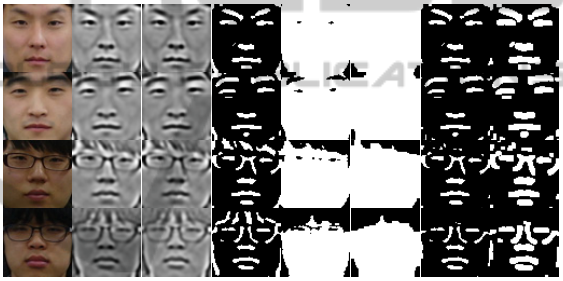

(a) (b) (c) (d) (e) (f) (g) (h)

Figure 2: (a) Original images (b) illumination normalized images (c) global intensity shifted images (d) binary images (e) facial regions obtained from YCbCr colour space based skin colour model (f) face region estimation (g) AND operation of (d) and (f) (h) dilation operation

3.2 Global Intensity Shifting & Image Binarization

After contrast equalization, the average intensities of the processed images differed slightly, as shown in Fig. 2c. The last person with glasses displayed low intensity pixels. Backgrounds, glasses, or hair styles affect contrast equalization since the procedure has to be applied to the entire image. To allow for these variations, we shifted the average intensity of each image so that each image showed a specific value:

$$I_s(x,y) = I(x,y) + \left(\mu - \frac{\Sigma_{x',y' \text{ in } I} I(x',y')}{\Sigma_{x',y' \text{ in } I} 1}\right). \quad (1)$$

where $I(x,y)$ and $I_s(x,y)$ represent pixel intensity values at a point (x,y) of image I and shifted image I_s. We calculated the average intensity values of all the illumination normalized facial images and

obtained $\mu = 135$. Then, we used this result as a reference so that the shifted image I_s showed the same average intensity value. Finally, binary images I_b were produced as follows:

$$I_b(x,y) = \begin{cases} 1, & 0 \le I_s(x,y) \le T \\ 0, & \text{otherwise} \end{cases} \quad (2)$$

The threshold point was empirically set to $T = 109$ so that each binary image retained important facial features such as eyes, eyebrows, a nose tip and a mouth (Fig. 2d). However, outlines of faces, hairs and glasses still appeared in the binary images.

3.3 Face Region Estimation

The YCbCr skin colour model (Chai and Ngan, 1999) was used for face region estimation. A transformation matrix was used to convert the RGB space to an YCbCr colour space as follows:

$$\begin{bmatrix} Y(x,y) \\ C_b(x,y) \\ C_r(x,y) \end{bmatrix} = \begin{bmatrix} 16 \\ 128 \\ 128 \end{bmatrix} + \begin{bmatrix} 65.758 & 129.057 & 25.064 \\ -37.945 & -74.494 & 112.439 \\ 112.439 & -94.154 & -18.285 \end{bmatrix} \begin{bmatrix} R(x,y) \\ G(x,y) \\ B(x,y) \end{bmatrix} \quad (3)$$

$$\text{Face}(x,y) = \begin{cases} 1, 77 \le C_b(x,y) \le 127,\ 133 \le C_r(x,y) \le 173 \\ 0, \text{otherwise} \end{cases} \quad (4)$$

Then, applying (4) to the YCbCr images produced face candidate regions, as shown in Fig. 2e. A morphological closing operation was used to fill the holes in the candidate regions. Here we adopted a 5×5 square template for the closing operation (Fig. 2f). Then, by using the candidate regions, the unnecessary parts (e.g., hair, face outline, etc.) were partially removed (Fig. 2g). Lastly, a 3×3 dilation operation was applied to reduce the effect of head pose variations (Fig. 2h).

4 SIMILARITY CALCULATION

4.1 Choosing Reference Images

We assumed that each reference image was captured and cropped to show all the necessary facial features including eyes, eyebrows, a nose tip, and a mouth. The size of the reference image had to be small enough to be fit in a limited packet size, since we assumed that mobile devices use a limited data transfer channel for initializing connections between devices. A 64×64 binary image was chosen for the reference images since it only needed 512 bytes to preserve the details of the facial features. In general, several image compression algorithms such as RunLength Encoding or Deflate can be used to compress binary images.

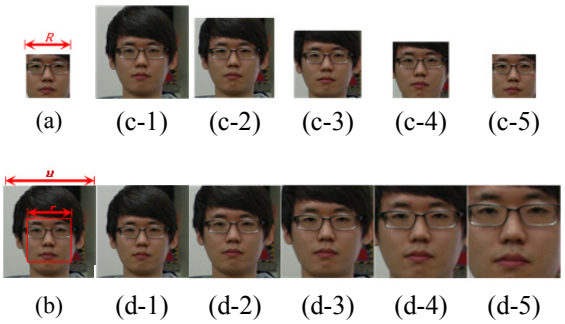

Figure 3: (a) The width of a reference image $R = 64$ (b) the width of a user selected test image u and the corresponding minimum face area of a test image r (c-1) $u : r = 2 : 1$ (c-2) $u : r = 1.75 : 1$ (c-3) $u : r = 1.5 : 1$ (c-4) $u : r = 1.25 : 1$ (c-5) $u : r = 1 : 1$ (d) The width of user cropped images were fixed with $u = 128$.

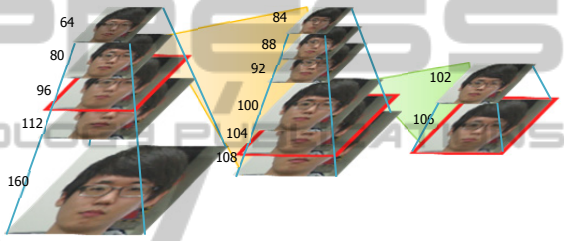

Figure 4: Scale Pyramids (Lowe, 1999) for each test image were constructed into three steps.

4.2 Scale Pyramids

The scale of a test image differs depending on camera settings: resolution, distance, lens, and zooming. Thus, image registration had to be performed for the test images at multiple scales.

Scale pyramids (Lowe, 1999) were used in our image registration scheme. We let R, u and r denote the width of a reference image, the width of a user cropped test image and the width of the minimum face area of a test image, respectively (Figs. 3a-b). It is obvious that r should be larger than R. As mentioned above, a user can crop a test image in various ways (Fig. 3c). Thus, we assumed that the ratio of u and r did not exceed 2.5.

To reduce the registration time, we constructed 3-step scale pyramids with different width intervals (Fig. 4). After performing image registration at 15 different scales, we chose the highest correlation score.

4.3 XNOR+AND Correlation

We let I_r and I_t denote the reference data set and the

test data set, respectively. Then, the Pearson product-moment correlation coefficient r between I_r and I_t was calculated by

$$r = \frac{n\sum I_r(x,y)I_t(x,y) - \sum I_r(x,y)\sum I_t(x,y)}{\sqrt{n\sum I_r^2(x,y) - (\sum I_r(x,y))^2}\sqrt{n\sum I_t^2(x,y) - (\sum I_t(x,y))^2}} \quad (5)$$

where x and y denote the pixel position and n is the number of pixels. We simplified this as the phi coefficient (Guilford, 1941) if the bit depth of I_r and I_t were 1 (i.e. binary image). However, calculating the Pearson product-moment correlation coefficient required high cost operations. Thus, we proposed a new correlation score method, XNOR+AND correlation score u, as follows:

$$u = \sum \neg\left(I_r(x,y) \downarrow I_t(x,y)\right) + \sum\left(I_r(x,y) \wedge I_t(x,y)\right) \quad (6)$$

where $\neg(A \downarrow B)$ and $(A \wedge B)$ denote the XNOR and AND operation, respectively. Since the range of u varied between 0 and $2n$, u was normalized by

$$U = \frac{u}{2n} \quad (7)$$

If the reference image is fixed, this normalization can be skipped for faster computation. Both the XNOR and AND operations presented correlations between two binary images. The XNOR operation showed information about the overlapping areas of both the face feature regions (1s) and the non-face feature regions (0s). On the other hand, the AND operation considered only the face feature regions. The non-face feature regions (0s) also provided information on the overall face shape. However, the AND operation considered only the facial regions. On the other hand, the XNOR operation considered both facial and non-facial regions. However, noise areas in the facial regions and those in the non-facial feature regions were treated equally. By using both the AND operation and the XNOR operation, noise areas in the non-face feature regions had fewer influences on the correlation score estimation.

4.4 Head Pose Variation Compensation

Head pose estimation is one of the important issues in face recognition. 3D model-based methods, learning-based methods and active appearance models are frequently used for pose-invariant face recognition. However, these methods were not suitable since reference sets continuously vary and the necessary long processing times may not be useful with mobile devices.

We assumed that a small amount of head rotations in yaw and pitch angles can be ignored by using binary images. Also, a dilation operation was applied to minimize the small differences in the pose variations. The proposed XNOR+AND score was robust against these head pose variations.

(a) (b) (c) (d) (e)

Figure 5: Cropped facial images taken from original images of Samsung Galaxy S3 (upper row), Sky Vega X (middle row) and Samsung NX10 (lower row). (a) frontal face (b) -15 ~ -45˚ yaw (c) +15 ~ +45˚ yaw (d) -15 ~ -45˚ pitch (e) +15 ~ +45˚ pitch angle tilted.

5 EXPERIMENTS

All the reference images were manually cropped to 64×64 pixels. The test image sizes were generally larger than those of the reference images. Recognition rates of gray images (8-bit images) with and without the pre-processing procedures are shown below for comparison.

Our test database consisted of 135 indoor facial images taken from two mobile phones and a DSLR camera. There were nine subjects with five different head poses, including frontal faces. As shown in Fig. 5, 15 facial images were taken for each person and they sometimes contained blurred images.

Table 1 shows a performance comparison. Scale pyramid image registration was applied to all the methods. The proposed method with the XNOR+AND similarity measure achieved the best overall performance (85.93%). The proposed method also showed the best performance among all pose variations. With the grayscale images, which were produced from the RGB images without the pre-processing procedure, the overall accuracy was 61.48%. When the pre-processing procedure was used (Tan and Triggs 2007), the overall accuracy improved to 68.15%. When the Pearson correlation was used, the overall recognition rate was 83.7%.

Table 1: Recognition performances achieved when enrolling one frontal face image.

Methods	Bit Depth	Criteria	Recognition Rates (%)						Processing Time (sec/image)
			f	-y	+y	-p	+p	Overall	
Grayscale	8	Pearson	100.00	33.33	40.74	70.37	62.96	61.48	2.156
(Tan and Triggs, 2007)	8	Pearson	88.89	62.96	66.67	62.96	59.26	68.15	2.421
Proposed method	1	Pearson	96.30	77.78	85.19	81.48	77.78	83.70	0.705
	1	XNOR+AND	96.30	85.19	85.19	81.48	81.48	85.93	0.575

6 CONCLUSIONS

In this paper, we proposed a link selection method for mobile device communications. Potential target devices broadcasted their ID features extracted from the owners' faces. Then, a user connected a target device by selecting the target device owner's face from his/her device display. We proposed an efficient matching method that used pre-processing, binarization and a simplified similarity measure. The experimental results were promising.

ACKNOWLEDGEMENTS

This research was funded by the MSIP (Ministry of Science, ICT & Future Planning), Korea in the ICT R&D Program 2013.

REFERENCES

Chai, D., Ngan, K. N., 1999. Face segmentation using skin-color map in videophone applications. *Circuits and Systems for Video Technology, IEEE Transactions on, 9*(4), 551-564.

Colmenarez, A. J., Huang, T. S., 1997. Face detection with information-based maximum discrimination. In *Computer Vision and Pattern Recognition, 1997. Proceedings., 1997 IEEE Computer Society Conference on* (pp. 782-787). IEEE.

Haartsen, J., 1998. Bluetooth-The universal radio interface for ad hoc, wireless connectivity. *Ericsson review, 3*(1), 110-117.

Guilford, J. P., 1941. The phi coefficient and chi square as indices of item validity. *Psychometrika, 6*(1), 11-19.

Lowe, D. G., 1999. Object recognition from local scale-invariant features. In *Computer Vision, 1999. The proceedings of the seventh IEEE international conference on* (Vol. 2, pp. 1150-1157). IEEE.

O'sullivan, J. D., Daniels, G. R., Percival, T. M., Ostry, D. I., Deane, J. F., 1996. *U.S. Patent No. 5,487,069*. Washington, DC: U.S. Patent and Trademark Office.

Tan, X., Triggs, B., 2007. Enhanced local texture feature sets for face recognition under difficult lighting conditions. In *Analysis and Modeling of Faces and Gestures* (pp. 168-182). Springer Berlin Heidelberg.

Zimmerman, T. G., 1996. Personal area networks: near-field intrabody communication. *IBM Systems Journal, 35*(3.4), 609-617.